



OPEN ACCESS

EDITED BY

Ute Gschwandtner,
University Hospital of Basel, Switzerland

REVIEWED BY

Leila Montaser-Kouhsari,
Stanford University, United States
Sagar Vyavahare,
Augusta University, United States

*CORRESPONDENCE

Aaron J. Suminski
✉ suminski@neurosurgery.wisc.edu

†These authors have contributed equally
to this work

RECEIVED 06 November 2025

REVISED 02 February 2026

ACCEPTED 09 February 2026

PUBLISHED 03 March 2026

CITATION

Moshchin M, Haebig MB, Luu CP,
Dean DC III, McMillan AB, Alexander AL,
Hurley SA, Gallagher CL and
Suminski AJ (2026) Separable, symptom
specific alterations in brain
microstructure associated with
early-stage Parkinson's disease.
Front. Neurosci. 20:1741159.
doi: 10.3389/fnins.2026.1741159

COPYRIGHT

© 2026 Moshchin, Haebig, Luu, Dean,
McMillan, Alexander, Hurley, Gallagher
and Suminski. This is an open-access
article distributed under the terms of the
[Creative Commons Attribution License
\(CC BY\)](https://creativecommons.org/licenses/by/4.0/). The use, distribution or
reproduction in other forums is
permitted, provided the original author(s)
and the copyright owner(s) are credited
and that the original publication in this
journal is cited, in accordance with
accepted academic practice. No use,
distribution or reproduction is permitted
which does not comply with these terms.

Separable, symptom specific alterations in brain microstructure associated with early-stage Parkinson's disease

Mikhail Moshchin^{1,2}, Maureen B. Haebig³, Cuong P. Luu^{1,2},
Douglas C. Dean III^{4,5,6}, Alan B. McMillan^{5,7},
Andrew L. Alexander^{5,6,8}, Samuel A. Hurley^{5,7},
Catherine L. Gallagher^{3,9†} and Aaron J. Suminski^{1,2*†}

¹Department of Neurological Surgery, University of Wisconsin-Madison, Madison, WI, United States,

²Wisconsin Institute for Translational Neuroengineering, University of Wisconsin-Madison, Madison, WI, United States,

³Department of Neurology, University of Wisconsin-Madison, Madison, WI, United States,

⁴Department of Pediatrics, University of Wisconsin-Madison, Madison, WI, United States,

⁵Department of Medical Physics, University of Wisconsin-Madison, Madison, WI, United States,

⁶Waisman Center, University of Wisconsin-Madison, Madison, WI, United States,

⁷Department of Radiology, University of Wisconsin-Madison, Madison, WI, United States,

⁸Department of Psychiatry, University of Wisconsin-Madison, Madison, WI, United States,

⁹William S. Middleton Memorial Veterans Hospital, Madison, WI, United States

Introduction: Parkinson's Disease (PD) is diagnosed based on motor symptoms (bradykinesia, resting tremor, rigidity); yet non-motor symptoms such as sleep abnormalities, autonomic dysfunction, and cognitive changes often precede motor signs, fulfilling the criteria for prodromal PD. How motor and non-motor symptoms emerge from dopamine depletion and whether they involve separable neural substrates remains unclear.

Methods: We applied correlational tractography based on multi-shell, diffusion-weighted magnetic resonance imaging in early-stage PD to assess microstructural changes throughout the brain. Eight participants with early-stage PD and 5 healthy controls underwent motor, cognitive, and mood assessments, followed by structural and multi-shell, diffusion-weighted magnetic resonance imaging. Their groupwise differences in white matter integrity associated with PD status were quantified using correlational tractography, with and without age correction.

Results: Correlational tractography delineated both microstructural changes that held either a significant positive or negative association with PD status, where the statistical maps of these changes linked differentially to motor and non-motor symptoms. Quantitative anisotropy (QA) extracted from positively associated fibers significantly correlated with cognitive function, while QA of negatively associated fibers correlated with motor function—independent of the effect of age. Of note, QA of positively associated fibers correlated with depressive mood only in the age-uncorrected analyses, suggesting a strong age-related effect.

Conclusion: In early-stage PD, motor and non-motor symptoms are mapped to anatomically distinct pathways, suggesting separable pathophysiological mechanisms. These findings further suggest that correlational tractography is appropriate to evaluate changes in structural connectivity in neurodegenerative diseases and, potentially, their therapeutic interventions.,

KEYWORDS

diffusion imaging, MRI, non-motor symptoms, Parkinson's disease, prodromal

Introduction

Parkinson's Disease (PD) is a progressive neurodegenerative disease affecting over 6 million people worldwide. Diagnosed primarily as a movement disorder, PD presents with motor symptoms that canonically include resting tremor, rigidity, and bradykinesia. Motor symptom onset coincides with the degeneration of dopamine-producing neurons in the substantia nigra pars compacta (SNc), resulting in striatal dopamine deficiency (Poewe et al., 2017). However, recent pathologic studies have revealed that SNc dopamine depletion is preceded by the accumulation of Lewy bodies in the myenteric plexus, olfactory bulb, limbic system, brainstem nuclei, and cerebral cortex (Braak et al., 2002). These findings putatively explain the non-motor symptoms that frequently emerge long before the appearance of motor symptoms, including gastrointestinal issues, olfactory dysfunction, sleep disturbances, depression, anxiety, pain, and fatigue (Kalia and Lang, 2015). These non-motor symptoms are equally disabling, and they fulfill the criteria for prodromal PD (Berg et al., 2015). Thus, there is a critical need to understand the interaction between the motor and non-motor symptoms of PD, especially how they might be instantiated within separable neural substrates.

Our understanding of PD pathophysiology and treatment (Horn et al., 2017; Rajamani et al., 2024) has advanced significantly, thanks to the development of advanced imaging techniques (Alexander et al., 2007). In particular, imaging reinforced the idea that PD is a disorder of brain networks that profoundly affects brain structure (Agosta et al., 2014; Duncan et al., 2016), function (Olde Dubbelink et al., 2014), and metabolism (Pappata et al., 2011; Poston and Eidelberg, 2010). For instance, structural studies have shown that, in PD, white matter microstructural integrity loss exceeds that of normal aging and correlates with cognitive symptoms (Gallagher et al., 2013; Pozorski et al., 2018). Furthermore, a longitudinal [18F]-fluorodeoxyglucose (FDG) positron emission tomography (PET) study associated mild PD with the activation of two networks with gain and loss of metabolic connections (Tang et al., 2024). Along with these human studies, preclinical models corroborate that alterations in a broad brain network are hallmarks of PD (see Cenci and Björklund, 2020 for review). Our own recent animal work showed that unilateral dopamine depletion leads to microstructural changes in at least two brain networks: one directly related to loss of nigrostriatal dopamine neurons and the other associated with the subsequent compensatory responses (Moshchin et al., 2025). Based on this evidence, we hypothesize that similar network

changes could be demonstrated in humans using comparable techniques.

Correlational tractography, a subdivision of connectometry, offers a promising way to evaluate network changes in PD (Yeh et al., 2016a). Unlike techniques assessing end-to-end connections between large parcellated volumes, correlational tractography tracks local connectivity changes to identify fiber tract segments strongly associated with structural, physiological, or behavioral measures. Previous human studies using this approach have focused primarily on motor function within regions-of-interest rather than network-based analyses. When comparing mild PD patients to healthy controls, Wen et al. found significantly lower QA in the corpus callosum, external capsule, cortico-thalamic tracts, and right corticospinal tract (Wen et al., 2016). Similarly, Sanchez-Catasus et al. showed impaired integrity of the dopaminergic nigrostriatal system in early-stage PD by combining correlational connectometry and 11C-dihydrotetrabenazine (11C-DTBZ) PET (Sanchez-Catasus et al., 2021). Kim et al. employed deterministic tractography based on quantitative anisotropy (QA) to link basal ganglia, cerebellum, and brainstem changes to motor symptoms, while changes in the temporal and occipital lobes correlated with olfactory dysfunction (Kim J. Y. et al., 2022). As noted, however, research has focused mainly on motor symptoms, with Kim et al. highlighting the need to explore cognitive decline and depression networks in early PD—crucial for developing effective treatments and improving patients' quality of life.

This early-stage pilot project utilized correlational tractography to identify white matter microstructural networks correlated with the disease state in early-stage PD patients and controls. We examined how motor and non-motor symptoms (i.e., cognitive flexibility, attention, and depressive mood) correlated with QA within identified networks. Two distinct networks emerged; each linked to either motor symptoms or non-motor symptoms. Notably, these symptom-specific network alterations closely parallel findings from our foundational preclinical study (Moshchin et al., 2025), suggesting conserved pathophysiological mechanisms across species and disease models.

Materials and methods

Participants

This pilot study recruited a total of 15 participants, 10 PD patients and 5 healthy controls, through the University of

Wisconsin Hospitals and Clinics. We selected PD patients with early-stage disease (Hoehn and Yahr stage = 2) and excluded those with (1) motor symptom onset before age 45; (2) a family history of PD in 2+ first-degree relatives; (3) atypical features including ataxic speech/limb/eye signs, supranuclear gaze abnormalities, apraxia, or myoclonus; (4) falls within 2 years of diagnosis; (5) significant cognitive impairment, fluctuating attention, or dementia; or (6) spontaneous hallucinations. For both the PD and control cohort, we further excluded those having (1) an implanted device incompatible with magnetic resonance imaging (MRI), (2) a significant central nervous system disease other than PD (e.g., multiple sclerosis, stroke, brain tumor), or (3) a history of a major psychiatric diagnosis (e.g., schizophrenia, bipolar affective disorder). Study procedures were approved by the University of Wisconsin Institutional Review Board (IRB # 2019–0987). Prior to participation, all participants demonstrated mental capacity and provided written informed consent in accordance with the declaration of Helsinki.

Motor and neuropsychological assessments

All participants underwent motor and cognitive assessments prior to MR imaging. Motor function of PD participants was evaluated while off-medication using the Unified Parkinson's Disease Rating Scale, Part III Motor Examination (UPDRS III) (Fahn and Elton, 1987). The non-motor aspects of PD were assessed while participants were on-medication using 3 tests: the Wisconsin Card Sort Test–64 Card Version to measure cognitive flexibility, working memory, and abstraction (lower score indicates fewer errors) (WCST-64) (Heaton, 1993); the Trail Making Test to evaluate visual attention and task switching (lower score indicates faster time) (TMT) (Reitan and Wolfson, 1993); and the nine-item Patient Health Questionnaire (PHQ-9) to assess the severity of depressive symptoms (lower score indicates lower severity) (Spitzer et al., 1999). Cohort differences in demographics and assessment scores were evaluated using two-sample *t*-tests in MATLAB (v2022a).

MRI acquisition and pre-processing

Following clinical assessments, brain MRIs were captured using a 3T GE SIGNA PET/MR scanner (GE HealthCare, Chicago, IL, United States) with a Nova 32-channel head coil (Nova Medical, Wilmington, MA, United States). In particular, we applied diffusion weighted imaging (DWI) with the following parameters: repetition time (TR) = 6,689 ms, echo time (TE) = 90.3 ms, matrix = 120 × 120, field of view (FOV) = 24 mm × 24 mm, isotropic voxel size = 2.0 × 2.0 × 2.0 mm³, multiband acceleration factor *R* = 3, in-plane acceleration = none, number of excitations (NEX) = 1, three shell acquisition with 9 directions at *b* = 300 s/mm², 18 directions at *b* = 850 s/mm², and 36 directions at *b* = 2,000 s/mm² (Δ = 12.20 ms, δ = 6 ms), with 10 *b* = 0 s/mm² acquisitions interleaved. Scans were repeated twice with reversed phase encoding gradient (AP and PA) to enable correction of susceptibility-induced distortions.

Image processing and connectometry analysis

DWI data were converted from the DICOM to NIfTI format using *dcm2nii* (Li et al., 2016), then corrected for distortion, eddy current, and motion using FSL TOPUP (Andersson et al., 2003) and EDDY (Andersson and Sotiropoulos, 2016; Jenkinson et al., 2012). As part of FSL EDDY preprocessing, in addition to eddy currents, volume-to-volume subject motion was also estimated for each diffusion encoding and a single image resampling was applied to correct for both susceptibility and subject motion-induced shifts in images. There was no significant difference in average frame-to-frame motion between the control (Mean ± Stdev: 0.2619 ± 0.1939 mm) and PD (0.2044 ± 0.0567 mm) cohorts (*p* = 0.411). All subsequent analyses were performed using DSI-Studio version Chen-2023-03-18 (Yeh et al., 2016a). We first examined the data for b-table orientation accuracy using an automatic quality control routine (Yeh et al., 2018). We then reconstructed the data in MNI space using q-space diffeomorphic reconstruction (Yeh and Tseng, 2011) to obtain the spin distribution function (Yeh et al., 2010) with a diffusion sampling of 1.25 and output isotropic resolution of 2.0 mm, employing the ICBM 152 Nonlinear Asymmetrical Template. Subsequently, local connectome matrices were estimated by sampling spin distribution function (SDFs) for each participant using the local fiber directions of the ICBM152 template. Diffusion was quantified using restricted diffusion imaging (Yeh et al., 2017), and quantitative anisotropy (QA) was extracted as a local connectome fingerprint for subsequent correlational tractography analyses (Yeh et al., 2016b). Sampling defined fiber directions within the ICBM152 template constrained diffusion metrics to biologically plausible streamlines.

Local connectome matrices (local connectome fingerprints) were assembled into a connectome database and analyzed using two approaches to assess PD-related connectivity changes (Yeh et al., 2016a). In the first, referred to as PD-Age, a non-parametric Spearman correlation evaluated the associations between the local connectome matrices and the PD status. In the second, referred to as PD+Age, a linear regression was first used to remove the effects of participant age on the diffusion data, and then a non-parametric Spearman correlation evaluated the associations between the local connectome matrices and the PD status without contribution from age. T-scores greater than 2.5 were tracked using a deterministic fiber tracking algorithm (Yeh et al., 2013) and filtered with 16 pruning iterations (Yeh et al., 2019). A false discovery rate (FDR) threshold of 0.05 was used to select tracts significantly associated with the disease state. Tracking used the following parameters: angular threshold = 15–90° selected pseudorandomly, step size 0.5–1.5 voxel selected pseudorandomly, and tracts shorter than 30 mm or longer than 200 mm were discarded. In total, 1,000,000 seeds were placed. To estimate the false discovery rate (FDR-corrected at *p* < 0.05), a total of 4000 randomized permutations were executed to estimate the null tract length distribution.

Furthermore, we wanted to explore if PD-related fiber tracts show symptom specificity; thus, we examined their association with motor and non-motor symptoms. Correlational tractography previously identified statistically significant and distinct fiber maps associated with the disease state. Now, in each of the PD-Age or PD+Age comparisons for each participant, we extracted the

mean QA value using the [Tracts][Statistics] function in DSI studio from all fiber tracts that showed a significant association—either positively or negatively—with the disease state. We then fit linear regression models (fitlm in MATLAB) to assess the relationship between the extracted QA values and motor, cognitive, or mood symptoms. Fits were considered significant if an *F*-test found the slope to be different from zero. Finally, we assessed connectivity patterns by calculating connection strength between regions of interest (ROIs) defined by the FreeSurferSeg Atlas in DSI-Studio. Connection strength was defined as the total number of tracts connecting two ROIs divided by the median length of those tracts. The resulting connectivity matrices from the PD-Age and PD+Age comparisons were superimposed to identify unique versus overlapping fiber tracts. The identity of white matter tracts was assessed using the HCP842 atlas within DSI-Studio.

Results

Demographics and cohort characteristics

Of the 15 participants, 13 had imaging data of sufficient quality for analysis (8 PDs and 5 controls; Table 1). One PD participant was excluded due to inconsistencies in the phase encoding directions of dMRI acquisitions; a second was excluded upon visual inspection of the reconstructed images, which did not adequately capture the cerebellum. PD enrollees were significantly younger than controls (Mean Age: 55.5 vs. 70.4, $p = 0.006$). As expected, PD participants also scored significantly higher on the UPDRS-III compared to controls (Mean score: 15.68 vs. 2.6, $p < 0.001$), reflecting degeneration in their motor function. The WCST-64, TMT (B-A), and PHQ-9 scores showed no significant difference between the PD and control cohorts.

Parkinson's disease modifies structural connectivity throughout the brain

This study aimed to investigate how PD impacts large white matter tracts using correlational tractography. We initially considered the effect of PD on brain microstructure without isolating the effect of participant age (PD-Age; Figure 1A). Here, correlational tractography showed broad, bilateral networks both positively and negatively associated with PD status. Positively associated fibers (Figure 1A, Red Fibers) included those in the bilateral prefrontal cortex (BA 10), the forceps minor, corticospinal tract connecting the midbrain, the sensorimotor cortex (BA1–4), and the cerebellar cortex. In contrast, negatively associated fibers (Figure 1A, Blue Fibers) were most prominent in the midbrain, with strong representation of fibers connecting the basal ganglia and thalamic nuclei. Interestingly, corticospinal tract fibers, distinct from those with a positive association, also showed negative associations with PD status.

Because our PD cohort was younger than controls (Table 1), we performed a second correlational tractography analysis controlling for participant age (PD+Age; Figure 1B). The PD+Age analysis found fewer positively correlated fibers associated with PD status compared to PD-Age (5,138 vs. 44,275 fibers, respectively), while

negatively associated fibers remained comparable (3,832 vs. 3,217 fibers, respectively). Importantly, similar network topography was preserved in both analyses, including: positively associated fibers in the bilateral frontal cortex/forceps minor, inferior frontal occipital fasciculus, inferior longitudinal fasciculus, corticospinal tract, and cerebellar peduncle/cortex; as well as negatively associated fibers in the basal ganglia, corticospinal tract, and inferior frontal occipital fasciculus.

When considering the pattern that emerged from the correlational tractography analyses (Figure 1), positively and negatively associated fibers showed largely distinct anatomical distributions with putatively different functional roles. Positively correlated fibers were predominantly located in higher-order cognitive regions of the prefrontal cortex, cerebellum, and precentral gyrus, whereas negatively correlated fibers were localized in subcortical structures, involving major white matter bundles and projection fibers. Therefore, following our previous preclinical PD work (Moshchin et al., 2025), we used linear regression to assess relationships between clinical symptom measures and QA values extracted from these fiber tracts (Figure 2). In the PD-Age analysis, positively associated fibers showed significant relationships (i.e., regression slopes) with executive function/attention [Trails (B-A), $T_{11} = 2.31$, $p = 0.04$, $R^2 = 0.33$; Figure 2A, Red Fibers] and depressive mood (PHQ-9, $T_{11} = 2.26$, $p = 0.045$, $R^2 = 0.32$; Figure 2A, Red Fibers). When controlling for age (PD+Age), the relationship with executive function/attention remained significant [Trails (B-A), $T_{11} = 2.42$, $p = 0.034$, $R^2 = 0.35$; Figure 2B, Red Fibers] but the depression association was lost (PHQ-9, $T_{11} = 0.84$, $p = 0.41$, $R^2 = 0.06$; Figure 2B, Red Fibers). We did not observe a significant relationship between the QA of positively correlated fibers and motor function (UPDRS-III) or cognitive flexibility (WCST-64) in either analysis. Interestingly, negatively associated fibers demonstrated significant relationships with motor symptoms in both analyses (PD-Age: UPDRS-III, $T_{11} = -2.67$, $p = 0.021$, $R^2 = 0.39$; Figure 2A, Blue Fibers) (PD+Age: UPDRS-III, $T_{11} = -2.33$, $p = 0.039$, $R^2 = 0.33$; Figure 2B, Blue Fibers). The QA of negatively correlated fibers did not show a significant relationship with measures of cognitive flexibility (WCST64), executive function/attention [Trails (B-A)], or depressive mood (PHQ-9) in either analysis.

Observing that the PD-Age and PD+Age analyses produced statistical maps with different representations of motor and non-motor symptoms (Figure 2), we then identified brain regions and fiber tracts that were conserved across analyses versus those unique to each analysis. For example, we posited that regions underlying motor disturbances would appear in negatively associated maps of both PD+Age and PD-Age, while depression-related regions would appear solely in the positively correlated map of PD-Age (Figure 3A). To pursue our goal quantitatively, we extracted separate connectivity matrices for positively and negatively correlated maps from the PD-Age and PD+Age analyses, superimposing them to assess unique versus overlapping connections (Figure 3B). We found that motor symptom-related regions were localized to overlapping negatively associated fiber tracts (Figure 3C and Supplementary Table 1, Negatively Associated) in the left hemisphere connecting the thalamus, putamen, and pallidum with the primary sensory/motor cortex via the corticospinal tract. These overlapping connections represented a total of 23% (6 of 26) negatively associated connections

TABLE 1 Characteristics of Parkinson's disease and control participants (mean \pm SEM).

Characteristic	PD ($n = 8$)	Control ($n = 5$)	T Stat (df)	p -value
Age (year)	55.5 \pm 2.86	70.4 \pm 3.09	3.44 (11)	0.006
Sex				
Male	6	3		N/A
Female	2	2		N/A
MDS-UPDRS (part III)	15.68 \pm 1.09	2.6 \pm 1.13	7.93 (11)	7.09e-06
Hoehn and Yahr stage	1.63 \pm 0.18	N/A		N/A
WCST-64 categories completed	3.25 \pm 0.62	2.0 \pm 0.45	1.44 (11)	0.178
Trail Making Tests (B-A)	32.88 \pm 5.47	30 \pm 5.47	0.35 (11)	0.740
Patient Health Questionnaire (PHQ-9)	3.88 \pm 1.08	1.2 \pm 0.73	1.79 (11)	0.100
PD duration (year)	5.5 \pm 1.57	N/A		
Daily L-Dopa equivalent dose (mg)	821.75 \pm 199.8	N/A		

df, degrees of freedom. Bold entries indicate statistical significance.

(Figure 3C). In contrast, executive/attentional dysfunction in PD was localized to overlapping positively associated fiber tracts (Figure 3C and Supplementary Table 1, Positively Associated). Here, these positively associated fibers totaled 35% (39 of 122) of connections and included both intra- and inter-hemispheric connections. Intrahemispheric connections included the right cerebellar cortex, right corticospinal tract linking subcortical structures to the primary motor cortex, a smaller portion of the left corticospinal tract innervating the primary motor cortex, and the right prefronto-caudate tract extending to the middle frontal and orbital gyrus. Overlapping interhemispheric connections were limited to forceps minor connecting the superior frontal gyrus and transverse frontopolar gyrus/sulcus. Because depressive mood was only related to positively associated fibers in the PD-Age analysis, we focused on the unique connections in the PD-Age statistical map to localize brain regions and fiber tracts that may directly relate to depressive mood (Figure 3B). The unique connections positively associated with PD-Age status (Figure 3A and Supplementary Table 2) included interhemispheric connections between (1) pons and bilateral cerebellar cortex via middle cerebellar peduncle, and (2) middle frontal gyrus/sulcus via forceps minor and accounted for 45% (50 of 119) of all connections.

Discussion

While PD is diagnosed based on motor dysfunction, early prodromal symptoms are nonspecific, manifesting as cognitive, olfactory, and gastrointestinal changes. Furthermore, the pathophysiology of these non-motor symptoms and their associated brain network changes remains less understood than that of motor symptoms. This study aimed to identify disease-correlated structural networks using diffusion-based correlational tractography during early-stage PD and examine how QA within these networks correlated with motor and non-motor symptoms.

Correlational tractography demonstrated separable statistical maps positively and negatively associated with PD status (Figure 1). QA within these networks showed differential relationships with motor and non-motor symptom severity, measured using

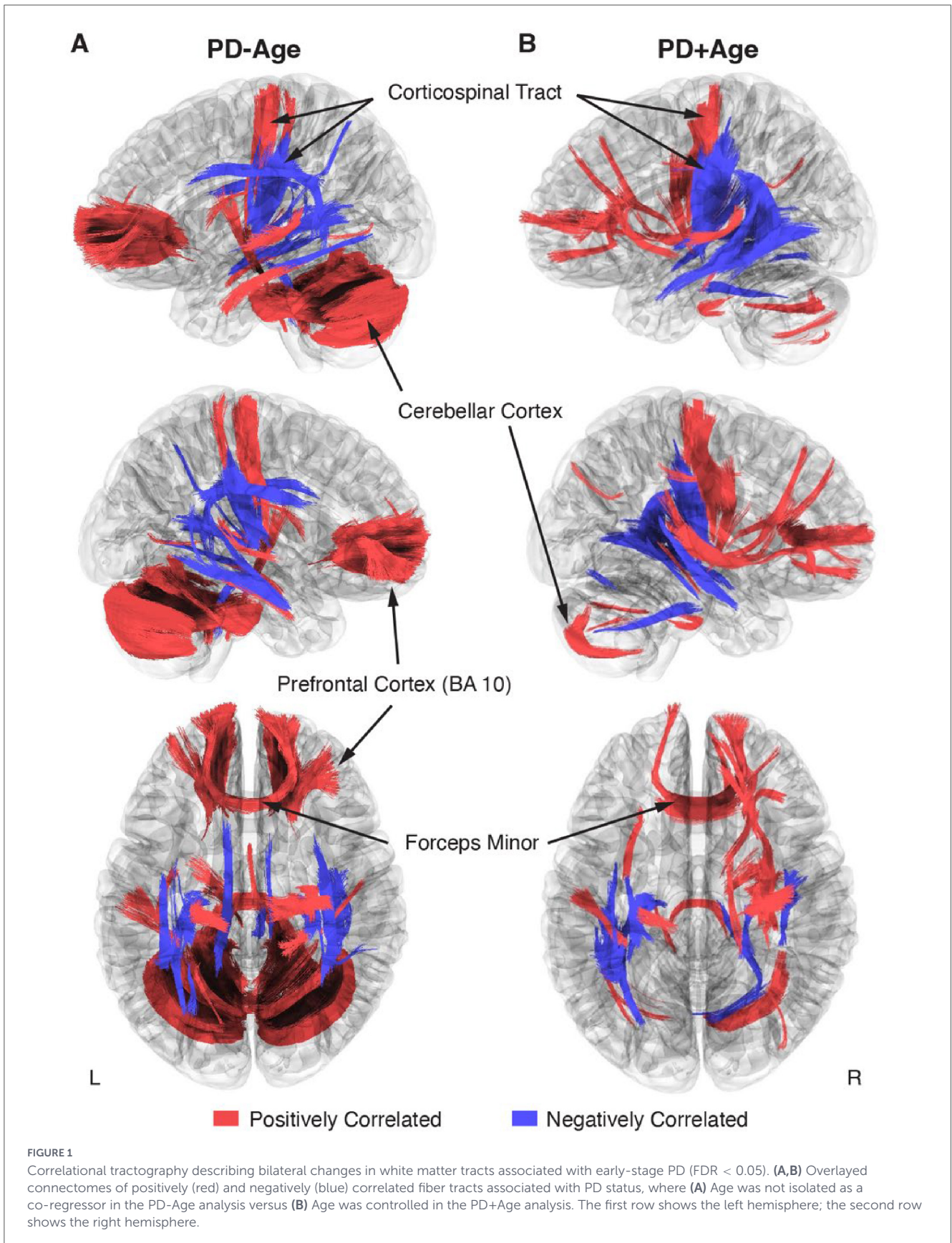
standardized clinical scales. Furthermore, cognitive dysfunction and depressive mood were associated with a specific network connecting the prefrontal cortex (BA10) bilaterally, the right prefrontal cortex (BA8), the basal ganglia, and the cerebellum. In contrast, motor dysfunction, measured by UPDRS-III, was correlated with regions/tracts showing negative association with the disease state, specifically linking the basal ganglia with the sensorimotor cortex via the corticospinal tract. Our findings suggest that structural white matter dysregulation/damage observed on correlational tractography may contribute to both non-motor (i.e., cognitive/depressive) and motor differences detected in early-stage PD patients.

Symptom-specific brain networks in PD

Numerous studies have reported associations between functional/structural alterations and clinical measures of both motor and non-motor symptoms (Andica et al., 2021; Gallagher et al., 2013; Kim J. et al., 2022; Pozorski et al., 2018; Sanchez-Catusus et al., 2021; Wen et al., 2016). For example, a recent longitudinal positron emission tomography (PET) study by Tang et al. illustrated the activation of two distinct brain networks, each characterized by either gain or loss of metabolic connections in early-stage PD (Tang et al., 2024). Consistent with Tang et al., our analysis in early-stage PD patients revealed two distinct statistical brain maps, one correlated with motor symptoms and the second with non-motor symptoms. Likewise, Kim, et al. showed that variations in QA within separable brain regions were selectively correlated with either motor or non-motor (i.e., olfactory) symptoms of PD. Notably, both age-controlled (PD+Age) and uncorrected (PD-Age) correlational tractography analyses revealed robust associations for motor and non-motor functions in similar brain regions, suggesting that these symptom-specific networks are independent of age effects.

Motor symptoms

We demonstrated that overlapping statistical network maps of motor symptoms in PD, maps common in both the PD-Age



and PD+Age analyses, were linked to negatively associated fiber tracts in the left hemisphere (Supplementary Table 1, Negatively Associated). These tracts connect the thalamus, putamen, and

pallidum with the primary sensory and motor cortex via the corticospinal tract, all of which play critical roles in motor control (Chu et al., 2024) and show well-recognized dysfunction

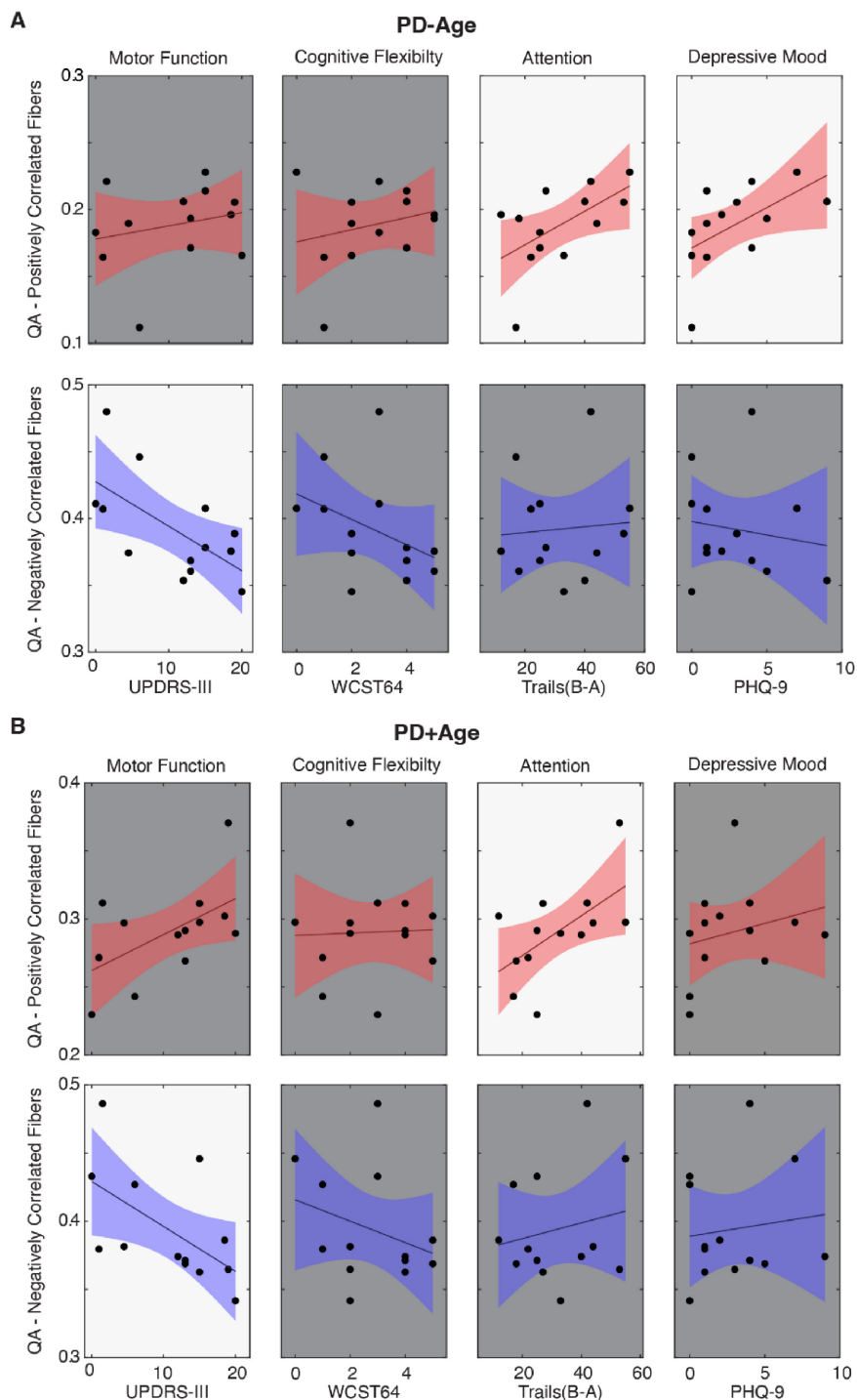


FIGURE 2

Linear regression models comparing mean QA values of fibers associated with PD status to clinical symptom measures. **(A,B)** UPDRS-III, Wisconsin Card Sort (WST64), Trail Making Tests (B-A), and Patient Health Questionnaire (PHQ-9) were correlated against mean QA of fibers associated with PD status, where the correlational tractography for QA in **(A)** did not isolate Age (PD-Age) and **(B)** controlled for Age (PD+Age). Red indicates fibers associated with increased QA in the early-stage PD cohort, and blue indicates fibers associated with decreased QA (FDR-corrected at $p < 0.05$). A bright background indicates statistical significance ($p < 0.05$).

in PD (see [Wichmann, 2019](#) for review). Our findings align with previous studies identifying motor-related structural changes. Interestingly, Kim et al. found that QA from the basal ganglia, brainstem, thalamus, and cerebellum most strongly correlated with motor symptoms (UPDRS-III) in early-stage PD; however, their analysis did not distinguish between individual nuclei, limiting

direct comparison. Similar to our study, Sanchez-Catusus et al. used correlational tractography to identify nigrostriatal fibers associated with striatal dopamine denervation measured by ¹¹C-dihydrotetrabenazine PET ([Sanchez-Catusus et al., 2021](#)). They showed that QA extracted from these fibers was negatively correlated with bradykinesia severity in patients with mild

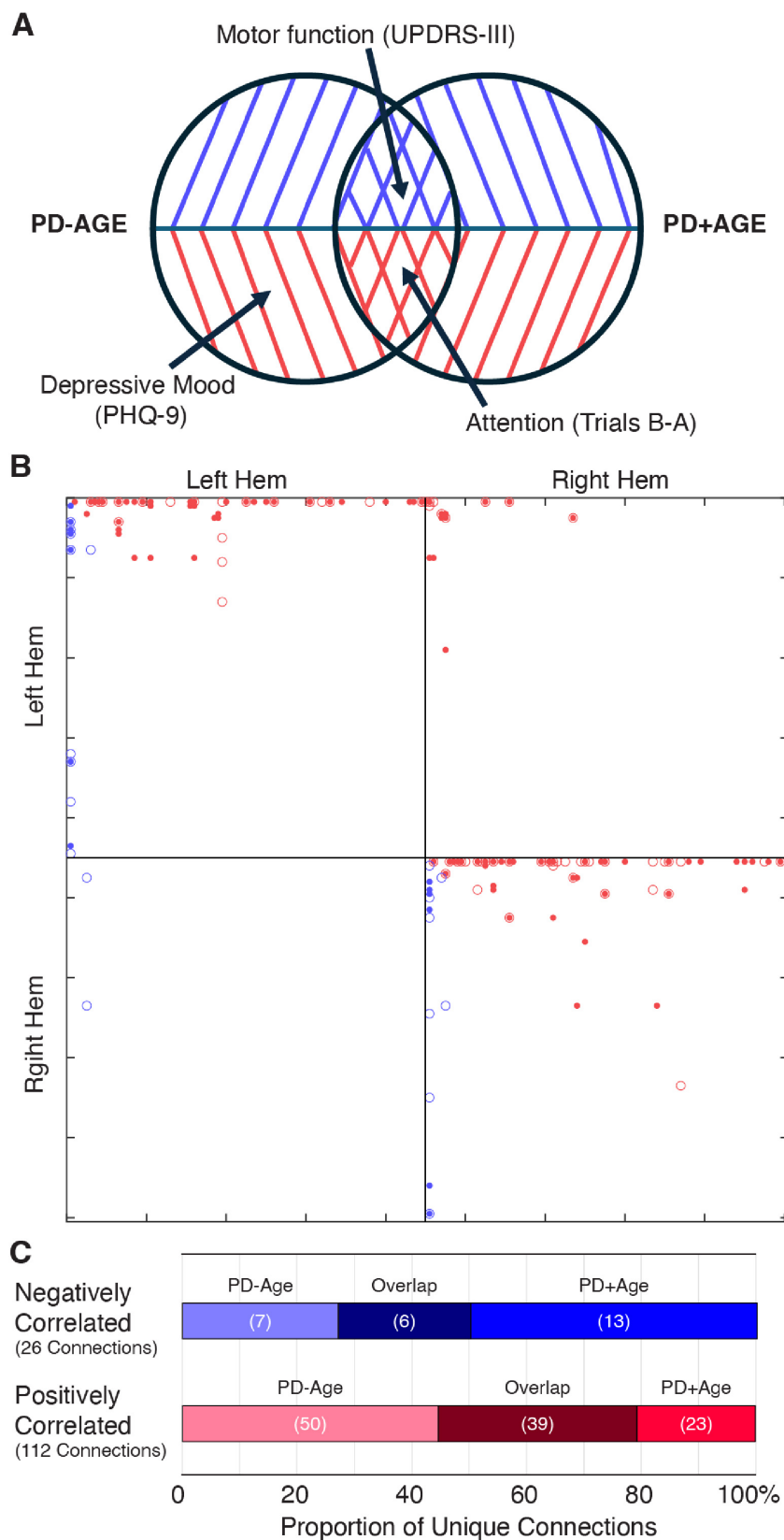


FIGURE 3

Connection patterns in positively and negatively associated statistical maps support symptom specificity. **(A)** Venn diagram illustrating unique versus overlapping connections from the statistical network maps of PD-Age and PD+Age analyses. **(B)** Connectivity matrices from correlational tractography using the FreeSurferSeg Atlas in DSI-Studio. Each marker represents tract connections between two regions of interest (ROIs), where: red indicates positively associated versus blue indicating negatively associated fiber tracts; dots represent PD-Age versus open circles representing PD+Age analysis results (age-controlled). **(C)** All unique connections (from each of the positively or negatively correlated groups) were further categorized based on whether they appeared solely in the PD-Age, solely in the PD+Age, or in both analyses (Overlap).

to moderate PD, suggesting that the reduced QA seen with increased disease severity reflects impaired axonal integrity in the nigrostriatal pathway. Our recent preclinical work corroborates the correlation between reduced QA and impaired integrity of the nigrostriatal dopamine pathway (Moshchin et al., 2025; Moshchin, 2023). Following unilateral 6-hydroxydopamine lesions in the median forebrain bundle (MFB), we showed that QA from the MFB strongly correlated with the degeneration of dopaminergic projections from the SNc to the striatum, measured via tyrosine hydroxylase staining. Taken together, these results demonstrate that impaired motor function in PD patients is strongly associated with degeneration of white matter tracts connecting the midbrain to the sensorimotor cortical areas. Future preclinical and clinical research should focus on the ability of this methodology to ascertain the efficacy of medical or neuromodulation therapy with the goal of optimizing patient specific interventions.

Non-motor symptoms

Similar to motor symptoms, we explored whether the statistical maps identified using correlational tractography carry significant correlations with non-motor symptoms of PD, including cognitive flexibility, attention, and depressive mood. We found no relationship between QA extracted from both positively and negatively associated maps with the WCST64, a measure of executive function. This is not surprising given that the decline on the WCST64 is most pronounced in late-stage PD (Lange et al., 2018), while our study cohort included only patients in early-stage PD.

In contrast, decreased attention/working memory function, measured by TMT, strongly correlated with QA extracted from fibers positively associated with PD status in both the PD-Age and PD+Age analyses. Though group-wise comparison of our two study cohorts did not show a significant difference in TMT (B-A), previous studies support attention/working memory dysfunction in PD patients (Kourtidou et al., 2015). Hanganu et al. found that PD patients with cognitive impairment exhibited increased diffusivity metrics in fiber bundles connecting the dorsolateral prefrontal cortex to subcortical structures, including the thalamus, caudate, and putamen (Hanganu et al., 2018). Similarly, using metabolic and structural studies in PD patients, Kubler et al. showed significant degeneration of frontostriatal networks and reduced metabolism in the prefrontal cortex, with TMT performance correlating with measures of prefrontal diffusion. In both PD+Age and PD-Age analyses, regions associated with deficits in attentional and executive control were most prominent within fiber tracts positively associated with PD (Supplementary Table 1, Positively Associated). Importantly, these included connections via the forceps minor that link the bilateral prefrontal cortex, specifically the superior frontal gyrus, the transverse frontopolar gyrus/sulcus, and the right prefronto-caudate tract. Indeed, Dirnberger et al. have put forth a plausible interpretation: dysfunction in the basal ganglia of PD patients, similar to our negatively correlated networks, necessitates compensatory recruitment of executive regions for tasks healthy individuals perform automatically—where the recruited fibers are represented by our “overlapping” positively associated fibers (Dirnberger and Jahanshahi, 2013).

Depression is strongly linked to PD (Cong et al., 2022; Schrag and Taddei, 2017; Wen et al., 2016). For example, a recent meta-analysis of > 38,000 subjects showed that one in three PD patients were diagnosed with depression. Multifactorial in origin, depression in PD seems to be strongly related to symptom severity and age of onset (Cong et al., 2022), more common with disabling axial motor symptoms like postural instability and gait disorders (Schrag and Taddei, 2017). Mood disorders have been linked to functional changes in limbic-cortical function, particularly in the subgenual cingulate and prefrontal cortex (Mayberg, 1997). Ansari et al. proposed that early depressive symptoms in PD are reactive responses to chronic degeneration, suggesting that the prefrontal and orbitofrontal cortices may be involved in early PD depression (Ansari et al., 2017). Furthermore, Prange et al. reported that depressive symptoms in early-stage PD patients are associated with altered diffusivity in the right limbic subnetwork, including the genu of the corpus callosum and the forceps minor (Prange et al., 2019). Importantly, these are the regions most targeted for deep brain stimulation in treatment-resistant depression (Lozano et al., 2008; Riva-Posse et al., 2014). Our data highlighted the correlation between depressive symptoms and the connections between (1) the middle frontal gyrus/sulcus via the forceps minor and (2) the pons and bilateral cerebellar cortex via the middle cerebellar peduncle (Figures 2, 3). Importantly, these connections were unique to PD-Age analysis and absent when controlling for age (PD+Age), aligning with past findings and reinforcing an age-dependent depression mechanism in early PD. The alignment with past findings regarding age further reinforces the validity of correlational tractography in detecting early-stage PD.

Limitations

Using correlational tractography, we demonstrated that structural changes in early-stage PD include two distinct networks associated with motor versus non-motor symptoms. However, there are a few important limitations. First, this is an early-stage pilot study that aims to explore whether correlational tractography based on multi-shell dMRI can identify symptom-specific brain networks in PD. As a result, we analyzed data from a small cohort ($n = 13$) of individuals with early-stage PD and healthy controls. The size of our study population and the unequal numbers of participants in each group presents potential confounds that should be addressed. Computation of FDR in our correlational tractography analysis is based on a permutation test where the null distribution is estimated by permuting the group labels. This, combined with use of residualization to control for any effects of participant age in the PD+Age analysis, introduces a risk of model instability/overfitting. Thus, our results should be interpreted through this lens pending future confirmatory studies with a larger sample size, age-matched cohorts, and greater diversity in age, lifestyles, PD symptoms (such as automatic dysfunctions, sleep disruptions, and sensory changes) and their severity, and clinical history will improve the generalizability of the results. Longitudinal follow-ups of such a study population using correlational tractography and predictive machine learning would also reveal deeper insight on PD progression and diagnostic biomarkers. That said, this report is timely given recent preclinical

work showing similar symptom-specific networks in the unilateral 6-OHDA animal model (Moshchin et al., 2025). Second, since our control cohort was significantly older than the PD cohort, age-related brain changes could have confounded the result. Indeed, both conventional indices like FA and MD extracted from diffusion tensor imaging and those, like QA, extracted from more advanced reconstruction methods are known to be sensitive to age (Liu et al., 2018; Schilling et al., 2022). Our analysis of both age-corrected and uncorrected networks, therefore, was designed to address this possible confound and to distinguish age-dependent from age-independent PD effects. Importantly, we found similar fiber maps in the two analyses. Third, we found that both positively and negatively associated fibers in our correlational tractography analyses were uniquely correlated with non-motor and motor symptoms of our participants. This is interesting given that non-motor effects, measured with TMT and PHQ-9, were not different between our control and PD groups. It is possible that the narrow range of possible scores in these measures could impact the stability of the correlations. We, however, note that there is a wide distribution of scores across participants (Figure 2, X-axis data); in all cases, these do not fall neatly into a simple PD versus healthy control categorization. Future confirmatory studies are necessary to validate the symptom specificity of these networks. Finally, we used the ICBM152 template derived from young adults; future studies should employ customized demographic-matched templates to improve accuracy and generalizability.

Data availability statement

The raw data supporting the conclusions of this article will be made available by the authors, without undue reservation.

Ethics statement

The studies involving humans were approved by the University of Wisconsin Institutional Review Board. The studies were conducted in accordance with the local legislation and institutional requirements. The participants provided their written informed consent to participate in this study.

Author contributions

MM: Writing – original draft, Visualization, Software, Data curation, Formal analysis, Validation, Writing – review & editing, Methodology. MH: Data curation, Writing – review & editing, Investigation, Validation, Formal analysis, Project administration. CL: Writing – review & editing, Investigation, Validation, Formal analysis, Visualization. DD: Writing – review & editing, Data curation, Methodology, Visualization. AM: Methodology, Writing – review & editing, Conceptualization, Validation, Funding acquisition, Resources. AA: Resources, Methodology, Validation, Writing – review & editing, Funding acquisition, Conceptualization. SH: Methodology, Software,

Writing – original draft, Investigation, Writing – review & editing, Visualization, Formal analysis, Validation, Resources, Data curation. CG: Funding acquisition, Resources, Writing – review & editing, Project administration, Writing – original draft, Methodology, Visualization, Data curation, Conceptualization, Validation, Supervision, Investigation. AS: Funding acquisition, Resources, Writing – review & editing, Writing – original draft, Formal analysis, Software, Methodology, Visualization, Supervision, Project administration, Conceptualization, Validation, Data curation.

Funding

The author(s) declared that financial support was received for this work and/or its publication. Support for this research was provided by NIH RO1AG08217 to CLG and the Departments of Radiology, Neurology and Neurological Surgery at the University of Wisconsin-Madison.

Conflict of interest

The author(s) declared that this work was conducted in the absence of any commercial or financial relationships that could be construed as a potential conflict of interest.

Generative AI statement

The author(s) declared that generative AI was not used in the creation of this manuscript.

Any alternative text (alt text) provided alongside figures in this article has been generated by Frontiers with the support of artificial intelligence and reasonable efforts have been made to ensure accuracy, including review by the authors wherever possible. If you identify any issues, please contact us.

Publisher's note

All claims expressed in this article are solely those of the authors and do not necessarily represent those of their affiliated organizations, or those of the publisher, the editors and the reviewers. Any product that may be evaluated in this article, or claim that may be made by its manufacturer, is not guaranteed or endorsed by the publisher.

Supplementary material

The Supplementary Material for this article can be found online at: <https://www.frontiersin.org/articles/10.3389/fnins.2026.1741159/full#supplementary-material>

References

- Agosta, F., Canu, E., Stefanova, E., Sarro, L., Tomić, A., Špica, V., et al. (2014). Mild cognitive impairment in Parkinson's disease is associated with a distributed pattern of brain white matter damage. *Hum. Brain Mapp.* 35, 1921–1929. doi: 10.1002/hbm.22302
- Alexander, A. L., Lee, J. E., Lazar, M., and Field, A. S. (2007). Diffusion tensor imaging of the brain. *Neurotherapeutics* 4, 316–329. doi: 10.1016/j.nurt.2007.05.011
- Andersson, J. L. R., Skare, S., and Ashburner, J. (2003). How to correct susceptibility distortions in spin-echo echo-planar images: Application to diffusion tensor imaging. *Neuroimage* 20, 870–888. doi: 10.1016/S1053-8119(03)00336-7
- Andersson, J. L. R., and Sotiropoulos, S. N. (2016). An integrated approach to correction for off-resonance effects and subject movement in diffusion MR imaging. *Neuroimage* 125, 1063–1078. doi: 10.1016/j.neuroimage.2015.10.019
- Andica, C., Kamagata, K., Saito, Y., Uchida, W., Fujita, S., Hagiwara, A., et al. (2021). Fiber-specific white matter alterations in early-stage tremor-dominant Parkinson's disease. *NPJ Parkinsons Dis.* 7:51. doi: 10.1038/s41531-021-00197-4
- Ansari, M., Rahmani, F., Dolatshahi, M., Pooyan, A., and Aarabi, M. H. (2017). Brain pathway differences between Parkinson's disease patients with and without REM sleep behavior disorder. *Sleep Breath.* 21, 155–161. doi: 10.1007/s11325-016-1435-8
- Berg, D., Postuma, R. B., Adler, C. H., Bloem, B. R., Chan, P., Dubois, B., et al. (2015). MDS research criteria for prodromal Parkinson's disease. *Mov. Disord.* 30, 1600–1611. doi: 10.1002/mds.26431
- Braak, H., Del Tredici, K., Bratzke, H., Hamm-Clement, J., Sandmann-Keil, D., and Rüb, U. (2002). Staging of the intracerebral inclusion body pathology associated with idiopathic Parkinson's disease (preclinical and clinical stages). *J. Neurol.* 249(Suppl. 3), iii1–iii5. doi: 10.1007/s00415-002-1301-4
- Cenci, M. A., and Björklund, A. (2020). Animal models for preclinical Parkinson's research: An update and critical appraisal. *Prog. Brain Res.* 252, 27–59. doi: 10.1016/bs.pbr.2020.02.003
- Chu, H.-Y., Smith, Y., Lytton, W. W., Grafton, S., Villalba, R., Masilamoni, G., et al. (2024). Dysfunction of motor cortices in Parkinson's disease. *Cereb. Cortex* 34:bhae294. doi: 10.1093/cercor/bhae294
- Cong, S., Xiang, C., Zhang, S., Zhang, T., Wang, H., and Cong, S. (2022). Prevalence and clinical aspects of depression in Parkinson's disease: A systematic review and meta-analysis of 129 studies. *Neurosci. Biobehav. Rev.* 141:104749. doi: 10.1016/j.neubiorev.2022.104749
- Dirnberger, G., and Jahanshahi, M. (2013). Executive dysfunction in Parkinson's disease: A review. *J. Neuropsychol.* 7, 193–224. doi: 10.1111/jnp.12028
- Duncan, G. W., Firbank, M. J., Yarnall, A. J., Khoo, T. K., Brooks, D. J., Barker, R. A., et al. (2016). Gray and white matter imaging: A biomarker for cognitive impairment in early Parkinson's disease? *Mov. Disord.* 31, 103–110. doi: 10.1002/mds.26312
- Fahn, S., and Elton, R. L. (1987). "Unified Parkinson's disease rating scale," in *Recent Developments in Parkinson's Disease*, Vol. 2, eds S. Fahn, C. D. Marsden, M. Goldstein, and D. B. Calne (Florham Park, NJ: Macmillan Healthcare Information), 153–163.
- Gallagher, C., Bell, B., Bendlin, B., Palotti, M., Okonkwo, O., Sodhi, A., et al. (2013). White matter microstructural integrity and executive function in Parkinson's disease. *J. Int. Neuropsychol. Soc.* 19, 349–354. doi: 10.1017/S1355617712001373
- Hanganu, A., Houde, J.-C., Fonov, V. S., Degroot, C., Mejia-Constain, B., Lafontaine, A.-L., et al. (2018). White matter degeneration profile in the cognitive cortico-subcortical tracts in Parkinson's disease. *Mov. Disord.* 33, 1139–1150. doi: 10.1002/mds.27364
- Heaton, R. K. (1993). *Wisconsin Card Sorting Test Computer Version 2*. Odessa, FL: Psychological Assessment Resources.
- Horn, A., Reich, M., Vorwerk, J., Li, N., Wenzel, G., Fang, Q., et al. (2017). Connectivity predicts deep brain stimulation outcome in Parkinson disease. *Ann. Neurol.* 82, 67–78. doi: 10.1002/ana.24974
- Jenkinson, M., Beckmann, C. F., Behrens, T. E. J., Woolrich, M. W., and Smith, S. M. (2012). FSL. *Neuroimage* 62, 782–790. doi: 10.1016/j.neuroimage.2011.09.015
- Kalia, L. V., and Lang, A. E. (2015). Parkinson's disease. *Lancet* 386, 896–912. doi: 10.1016/S0140-6736(14)61393-3
- Kim, J., Wichmann, T., Inan, O. T., and DeWeerth, S. P. (2022). Analyzing the effects of parameters for tremor modulation via phase-locked electrical stimulation on a peripheral nerve. *J. Pers. Med.* 12:76. doi: 10.3390/jpm12010076
- Kim, J.-Y., Shim, J.-H., and Baek, H.-M. (2022). White matter microstructural alterations in newly diagnosed Parkinson's disease: A whole-brain analysis using dMRI. *Brain Sci.* 12:227. doi: 10.3390/brainsci12020227
- Kourtidou, P., Kasselimis, D., Potagas, C., Zalonis, I., and Evdokimidis, I. (2015). Effects of mental flexibility and motor dysfunction on cognitive performance in patients with Parkinson's disease. *Arch. Neurosci.* 2:e21087. doi: 10.5812/archneurosci.21087
- Lange, F., Brückner, C., Knebel, A., Seer, C., and Kopp, B. (2018). Executive dysfunction in Parkinson's disease: A meta-analysis on the Wisconsin Card Sorting Test literature. *Neurosci. Biobehav. Rev.* 93, 38–56. doi: 10.1016/j.neubiorev.2018.06.014
- Li, X., Morgan, P. S., Ashburner, J., Smith, J., and Rorden, C. (2016). The first step for neuroimaging data analysis: DICOM to NIfTI conversion. *J. Neurosci. Methods* 264, 47–56. doi: 10.1016/j.jneumeth.2016.03.001
- Liu, X., Gao, X., Zhang, L., Yuan, Z., Zhang, C., Lu, W., et al. (2018). Age-related changes in fiber tracts in healthy adult brains: A generalized q-sampling and connectometry study. *J. Magn. Reson. Imaging* 48, 369–381. doi: 10.1002/jmri.25949
- Lozano, A. M., Mayberg, H. S., Giacobbe, P., Hamani, C., Craddock, R. C., and Kennedy, S. H. (2008). Subcallosal cingulate gyrus deep brain stimulation for treatment-resistant depression. *Biol. Psychiatry* 64, 461–467. doi: 10.1016/j.biopsych.2008.05.034
- Mayberg, H. S. (1997). Limbic-cortical dysregulation: A proposed model of depression. *J. Neuropsychiatry Clin. Neurosci.* 9, 471–481. doi: 10.1176/jnp.9.3.471
- Moshchin, M. (2023). "Quantifying changes in local basal ganglia structural connectivity in the 6-hydroxydopamine model of Parkinson's disease using correlational tractography," in *Proceedings of the 11th International IEEE/EMBS Conference on Neural Engineering (NER)*, (Baltimore, MD: IEEE). doi: 10.1109/ner52421.2023.10123839
- Moshchin, M., Schultz, R. J., Cheng, K. P., Osting, S., Koepfer, J., Luluzerne, M., et al. (2025). Assessing changes in whole-brain structural connectivity in the unilateral 6-hydroxydopamine rat model of Parkinson's disease using diffusion imaging and tractography. *J. Neural Eng.* 22:046005. doi: 10.1088/1741-2552/ade567
- Olde Dubbelink, K. T. E., Schoonheim, M. M., Deijen, J. B., Twisk, J. W. R., Barkhof, F., and Berendse, H. W. (2014). Functional connectivity and cognitive decline over 3 years in Parkinson disease. *Neurology* 83, 2046–2053. doi: 10.1212/WNL.0000000000001020
- Pappatà, S., Santangelo, G., Aarsland, D., Vicidomini, C., Longo, K., Bronnick, K., et al. (2011). Mild cognitive impairment in drug-naïve patients with PD is associated with cerebral hypometabolism. *Neurology* 77, 1357–1362. doi: 10.1212/WNL.0b013e3182315259
- Poewe, W., Seppi, K., Tanner, C. M., Halliday, G. M., Brundin, P., Volkman, J., et al. (2017). Parkinson disease. *Nat. Rev. Dis. Primers* 3:17013. doi: 10.1038/nrdp.2017.13
- Poston, K. L., and Eidelberg, D. (2010). FDG PET in the evaluation of Parkinson's disease. *PET Clin.* 5, 55–64. doi: 10.1016/j.pct.2009.12.004
- Pozorski, V., Oh, J. M., Adluru, N., Merluzzi, A. P., Theisen, F., Okonkwo, O., et al. (2018). Longitudinal white matter microstructural change in Parkinson's disease. *Hum. Brain Mapp.* 39, 4150–4161. doi: 10.1002/hbm.24239
- Prange, S., Metereau, E., Maillet, A., Lhommée, E., Klinger, H., Pelissier, P., et al. (2019). Early limbic microstructural alterations in apathy and depression in de novo Parkinson's disease. *Mov. Disord.* 34, 1644–1654. doi: 10.1002/mds.27793
- Rajamani, N., Friedrich, H., Butenko, K., Dembek, T., Lange, F., Navrátil, P., et al. (2024). Deep brain stimulation of symptom-specific networks in Parkinson's disease. *Nat. Commun.* 15:4662. doi: 10.1038/s41467-024-48731-1
- Reitan, R. M., and Wolfson, D. (1993). *The Halstead-Reitan Neuropsychological Test Battery: Theory and Clinical Interpretation*, 2nd Edn. Tucson, AZ: Neuropsychology Press.
- Riva-Posse, P., Choi, K. S., Holtzheimer, P. E., McIntyre, C. C., Gross, R. E., Chaturvedi, A., et al. (2014). Defining critical white matter pathways mediating successful subcallosal cingulate deep brain stimulation for treatment-resistant depression. *Biol. Psychiatry* 76, 963–969. doi: 10.1016/j.biopsych.2014.03.029
- Sanchez-Catasus, C. A., Bohnen, N. I., Yeh, F.-C., D'Cruz, N., Kanel, P., and Müller, M. L. T. M. (2021). Dopaminergic nigrostriatal connectivity in early Parkinson disease: In vivo neuroimaging study of 11C-DTBZ PET combined with correlational tractography. *J. Nucl. Med.* 62, 545–552. doi: 10.2967/jnumed.120.248500
- Schilling, K. G., Archer, D., Yeh, F.-C., Rheault, F., Cai, L. Y., Hansen, C., et al. (2022). Aging and white matter microstructure and macrostructure: A longitudinal multi-site diffusion MRI study of 1218 participants. *Brain Struct. Funct.* 227, 2111–2125. doi: 10.1007/s00429-022-02503-z
- Schrag, A., and Taddei, R. N. (2017). Depression and anxiety in Parkinson's disease. *Int. Rev. Neurobiol.* 133, 623–655. doi: 10.1016/bs.irn.2017.05.024
- Spitzer, R. L., Kroenke, K., and Williams, J. B. (1999). Validation and utility of a self-report version of PRIME-MD: The PHQ primary care study. Primary care evaluation of mental disorders. Patient health questionnaire. *JAMA* 282, 1737–1744. doi: 10.1001/jama.282.18.1737
- Tang, C. C., Nakano, Y., Vo, A., Nguyen, N., Schindlbeck, K. A., Mattis, P. J., et al. (2024). Longitudinal network changes and phenoconversion risk in isolated REM sleep behavior disorder. *Nat. Commun.* 15:10797. doi: 10.1038/s41467-024-54695-z
- Wen, M.-C., Chan, L. L., Tan, L. C. S., and Tan, E. K. (2016). Depression, anxiety, and apathy in Parkinson's disease: Insights from neuroimaging studies. *Eur. J. Neurol.* 23, 1001–1019. doi: 10.1111/ene.13002
- Wichmann, T. (2019). Changing views of the pathophysiology of Parkinsonism. *Mov. Disord.* 34, 1130–1143. doi: 10.1002/mds.27741

- Yeh, F.-C., Badre, D., and Verstynen, T. (2016a). Connectometry: A statistical approach harnessing the analytical potential of the local connectome. *Neuroimage* 125, 162–171. doi: 10.1016/j.neuroimage.2015.10.053
- Yeh, F.-C., Vettel, J. M., Singh, A., Poczos, B., Grafton, S. T., Erickson, K. I., et al. (2016b). Quantifying differences and similarities in whole-brain white matter architecture using local connectome fingerprints. *PLoS Comput. Biol.* 12:e1005203. doi: 10.1371/journal.pcbi.1005203
- Yeh, F.-C., Liu, L., Hitchens, T. K., and Wu, Y. L. (2017). Mapping immune cell infiltration using restricted diffusion MRI. *Magn. Reson. Med.* 77, 603–612. doi: 10.1002/mrm.26143
- Yeh, F.-C., Panesar, S., Barrios, J., Fernandes, D., Abhinav, K., Meola, A., et al. (2019). Automatic removal of false connections in diffusion MRI tractography using topology-informed pruning (TIP). *Neurotherapeutics* 16, 52–58. doi: 10.1007/s13311-018-0663-y
- Yeh, F.-C., Panesar, S., Fernandes, D., Meola, A., Yoshino, M., Fernandez-Miranda, J. C., et al. (2018). Population-averaged atlas of the macroscale human structural connectome and its network topology. *Neuroimage* 178, 57–68. doi: 10.1016/j.neuroimage.2018.05.027
- Yeh, F.-C., and Tseng, W.-Y. I. (2011). NTU-90: A high angular resolution brain atlas constructed by q-space diffeomorphic reconstruction. *Neuroimage* 58, 91–99. doi: 10.1016/j.neuroimage.2011.06.021
- Yeh, F.-C., Verstynen, T. D., Wang, Y., Fernández-Miranda, J. C., and Tseng, W.-Y. I. (2013). Deterministic diffusion fiber tracking improved by quantitative anisotropy. *PLoS One* 8:e80713. doi: 10.1371/journal.pone.0080713
- Yeh, F.-C., Wedeen, V. J., and Tseng, W.-Y. I. (2010). Generalized q-sampling imaging. *IEEE Trans. Med. Imaging* 29, 1626–1635. doi: 10.1109/TMI.2010.2045126